by HATs causes the remodeling of chromatin from a tightly to a loosely packed configuration, leading to transcriptional activation. Conversely, a decrease of histone acetylation by HDACs results in a condensed chromatin structure and thus suppresses transcription (Juliandi et al., 2010). Inhibition of HDAC activity by valproic acid (VPA), a widely used anticonvulsant and mood-stabilizing drug, has been shown to drive mESCs to differentiate into the ectodermal lineage at the expense of mesodermal and endodermal lineages (Murabe et al., 2007). This ectodermal lineage differentiation is further biased in favor of neuronal rather than glial fates by the VPA treatment (Murabe et al., 2007). Prior to this finding in mESCs, we and others (Hsieh et al., 2004; Balasubramaniyan et al., 2006) had also found a similar tendency for neuronal over glial fate preference when we cultured neural progenitor cells (NPCs) in the presence of HDAC inhibitors such as VPA and trichostatin A. The types of neurons produced in these studies were not examined in detail, however, and the effects of HDAC inhibition on the differentiation of mESC-derived NPCs have not yet been studied.

Here we report that HDAC inhibition in mESC-derived NPCs treated with VPA resulted in a recapitulation of later stages of corticogenesis. VPA treatment increased the production of cut-like homeobox 1 (Cux1)-positive superficial-layer neurons and decreased that of B-cell leukemia/lymphoma 11B (Bcl11b; also called Ctip2)-positive deep-layer neurons. These results suggest an important role of histone acetylation for the specification of superficial-layer neurons in late corticogenesis.

2. Materials and methods

2.1. Maintenance of mESCs

The mESC line 46C (*Sox1*-GFP-IRES-pac knock-in) was routinely propagated without feeder cells as described previously (Ying et al., 2003; Conti et al., 2005). mESCs were grown at 37 °C in a 5% (v/v) CO_2 incubator in ESC medium (ESM) containing Glasgow Minimum Essential Medium (Invitrogen), supplemented with 10% (v/v) fetal bovine serum (Biowest), 1 mM sodium pyruvate (Invitrogen), 0.1 mM MEM non-essential amino acids (Invitrogen), 0.1 mM 2-mercaptoethanol (Sigma), and 1000 U/ml murine leukemia inhibitory factor (Millipore), on 0.1% (v/v) gelatin-coated (Sigma) 9-cm dishes (Nunc). Medium was changed every day, and when the cells reached 60–70% confluence they were passaged onto new dishes at a plating density of 1×10^6 cells per 9-cm dish.

2.2. Neural differentiation

mESCs were induced to differentiate to the neural lineage as described previously (Ying et al., 2003; Conti et al., 2005; Gaspard et al., 2008, 2009). In brief, mESCs were trypsinized, dissociated and plated on 0.1% (v/v) gelatin-coated (Sigma) dishes at a density of 0.3×10^6 cells per 9-cm dish (Nunc) in ESM. One day later, the medium was replaced with DDM, which is composed of DMEM/F12 (Invitrogen) supplemented with freshly prepared modified N2-supplement (Ying and Smith, 2003), 1 mM sodium pyruvate (Invitrogen), 0.1 mM MEM non-essential amino acids (Invitrogen), 0.1 mM 2-mercaptoethanol (Sigma), 0.5 mg/ml bovine serum albumin fraction V (Invitrogen), 1× GlutaMAX (Invitrogen) and 0.5× antibiotic–antimycotic (Invitrogen). This day was designated as differentiation day 0. Cyclopamine (Calbiochem) was added to a final concentration of 1 μM from differentiation day 2 to day 10. On differentiation day 10, the medium was replaced with DDM only (without cyclopamine). For selection of Sox1-expressing neural progenitor cells, from differentiation day 8 to day 10, puromycin (Sigma) was added to a final concentration of 0.5 μg/ml. The culture was maintained until differentiation day 12 and the medium was changed every 2 days during day 0 to day 12.

At differentiation day 12, mESC-derived NPCs were trypsinized, dissociated and plated on poly-L-lysine/laminin-coated (Sigma, Becton Dickinson) dishes at a density of 0.5×10^6 cells per 3.5-cm dish (Nunc) in N2/B27 medium, which consists of a 1:1 mixture of DDM (without sodium pyruvate and MEM non-essential amino acids) and Neurobasal/B27 medium (Neurobasal, 1× B27 supplement without vitamin A, 1× GlutaMAX and 0.5× antibiotic–antimycotic (all from Invitrogen)). Valproic acid (Sigma) was added one time to the culture medium to a final concentration of 0.5 mM at differentiation day 12 where appropriate. Culture was maintained until differentiation day 14 or 21, and the medium was changed every 2 days during day 12 to day 21.

2.3. Immunocytochemistry

Medium was removed and cells were washed with phosphate buffered saline (PBS) and then fixed with 4% paraformaldehyde in PBS for 15 min. After 3 washes with PBS, the cells were incubated for 1 h at room temperature (RT) in blocking solution (PBS containing 3% FBS and 0.1% Triton X-100). They were then incubated overnight at 4 °C with the appropriate primary antibodies. The following primary antibodies were used: chick anti-GFP (1:500, Aves Labs), rabbit anti-β-tubulin isotype III (Tuj1; 1:1000, Covance), mouse anti-nestin (1:250, Millipore), rabbit anti-Pax6 (1:500, Covance), mouse anti-Map2ab (1:1000, Sigma), rat anti-Ctip2 (1:1000, Abcam), mouse anti-reelin (1:1000, MBL), and rabbit anti-Cux1 (1:500, Santa Cruz). After 3 washes with PBS, the cells were incubated for 2 h at RT with the appropriate secondary antibodies. The following secondary antibodies were used: FITC-conjugated donkey anti-chick, Cy5-conjugated donkey anti-rabbit, Cy3-conjugated donkey anti-rabbit, Cy5-conjugated donkey anti-mouse, Cy3-conjugated donkey anti-mouse (all 1:500, Jackson ImmunoResearch), Alexa Fluor 488-conjugated donkey anti-mouse, Alexa Fluor 488-conjugated donkey anti-rabbit, and Alexa Fluor 488-conjugated donkey anti-rat (all 1:500, Invitrogen). After 3 washes with PBS, nuclei were stained for 15 min at RT with Hoechst 33258 (Nacalai Tesque). Cells were washed with PBS, mounted on cover slips with Immu-Mount (Thermo Scientific), and examined and photographed using a fluorescence microscope (Axiovert 200M, Zeiss) equipped with a camera and appropriate epifluorescence filters.

3. Results

3.1. 46C mESCs differentiate into the neuroectodermal lineage under Shh inhibition

We used 46C mESCs, one of whose characteristic features is the replacement of the *Sox1* open reading frame with that encoding green fluorescent protein (GFP) (Ying et al., 2003). Since *Sox1* is the earliest known neuroectodermal marker in the mouse embryo (Pevny et al., 1998; Wood and Episkopou, 1999), we could follow neural commitment of 46C mESCs in culture by monitoring their GFP expression.

46C mESCs can differentiate efficiently into the neural lineage in feeder-free adherent monolayer culture supplemented with serum-free medium (Ying et al., 2003; Conti et al., 2005; Abranches et al., 2009). *Sox1*-GFP-expressing NPCs can be detected from differentiation day 2, and composed more than 75% of the total cell population at differentiation day 4 in N2/B27 medium (Ying et al., 2003). To assess the neural commitment of 46C mESCs in the adherent monolayer culture system proposed by Gaspard et al. (2008), we cultured these cells at low density in a chemically defined

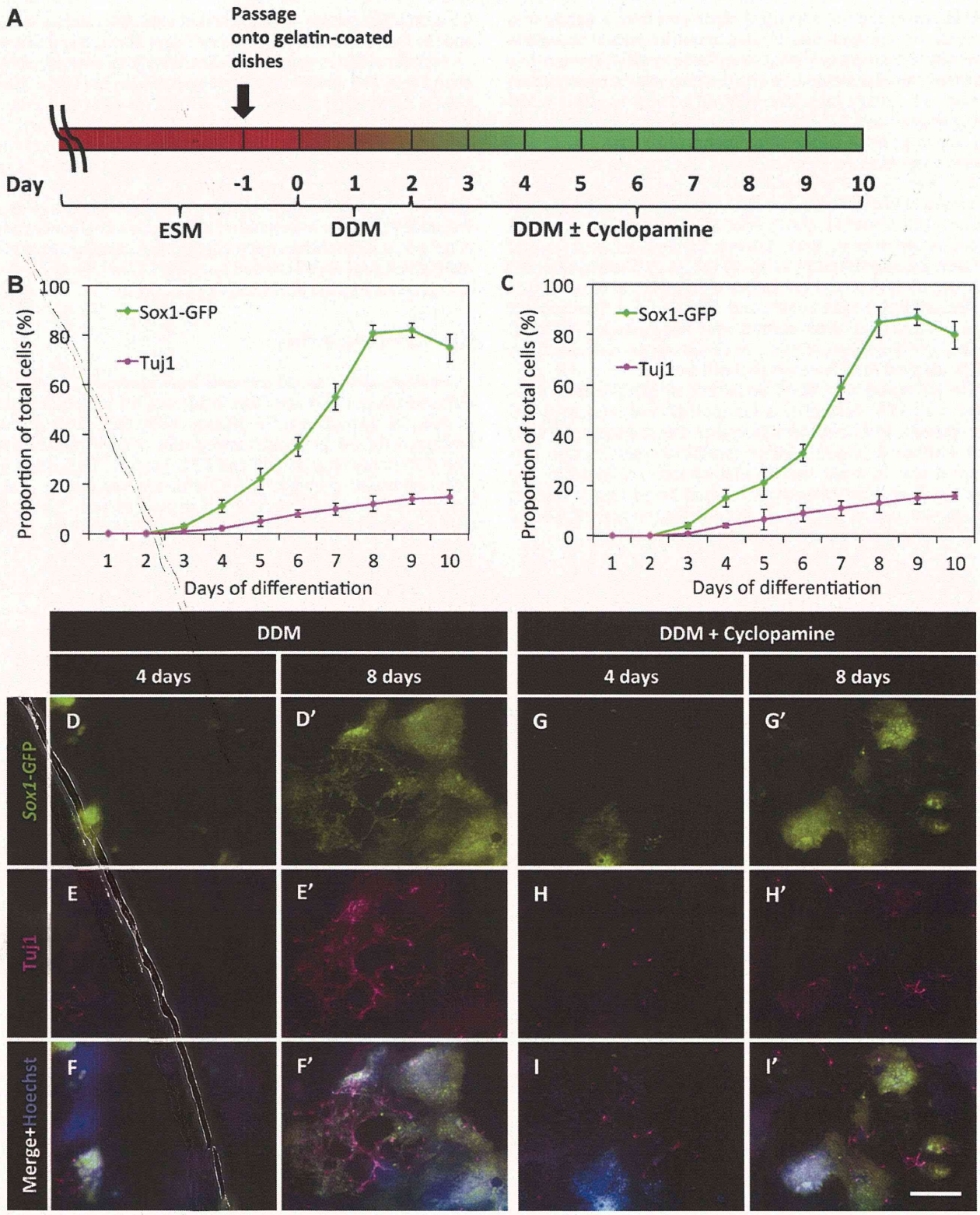

Fig. 1. 46C mESCs differentiate to the neuroectodermal lineage. (A) Timeline of the neural induction protocol using chemically defined default medium (DDM). mESCs were routinely propagated and then passaged to gelatin-coated dishes in embryonic stem cell medium (ESM) 1 day before neural induction (day −1). The next day (day 0), the medium was changed to DDM, and cyclopamine was added where appropriate from differentiation day 2 to day 10. The proportions of *Sox1*-GFP+ NPCs and Tuj1+ neurons did not differ in DDM (B) and in DDM with cyclopamine (C) during the culture period. Data are mean ± SD from at least three independent experiments. (D–I) Representative immunostaining images from differentiation day 4 and day 8 of *Sox1*-GFP-expressing (green in D, D′, G, and G′) and Tuj1-expressing (magenta in E, E′, H, and H′) cells, used for the quantitative data shown in B and C. Merged images with Hoechst (blue in F, F′, I, and I′) are also shown. Scale bar is 100 μm. (For interpretation of the references to color in this figure legend, the reader is referred to the web version of the article.)

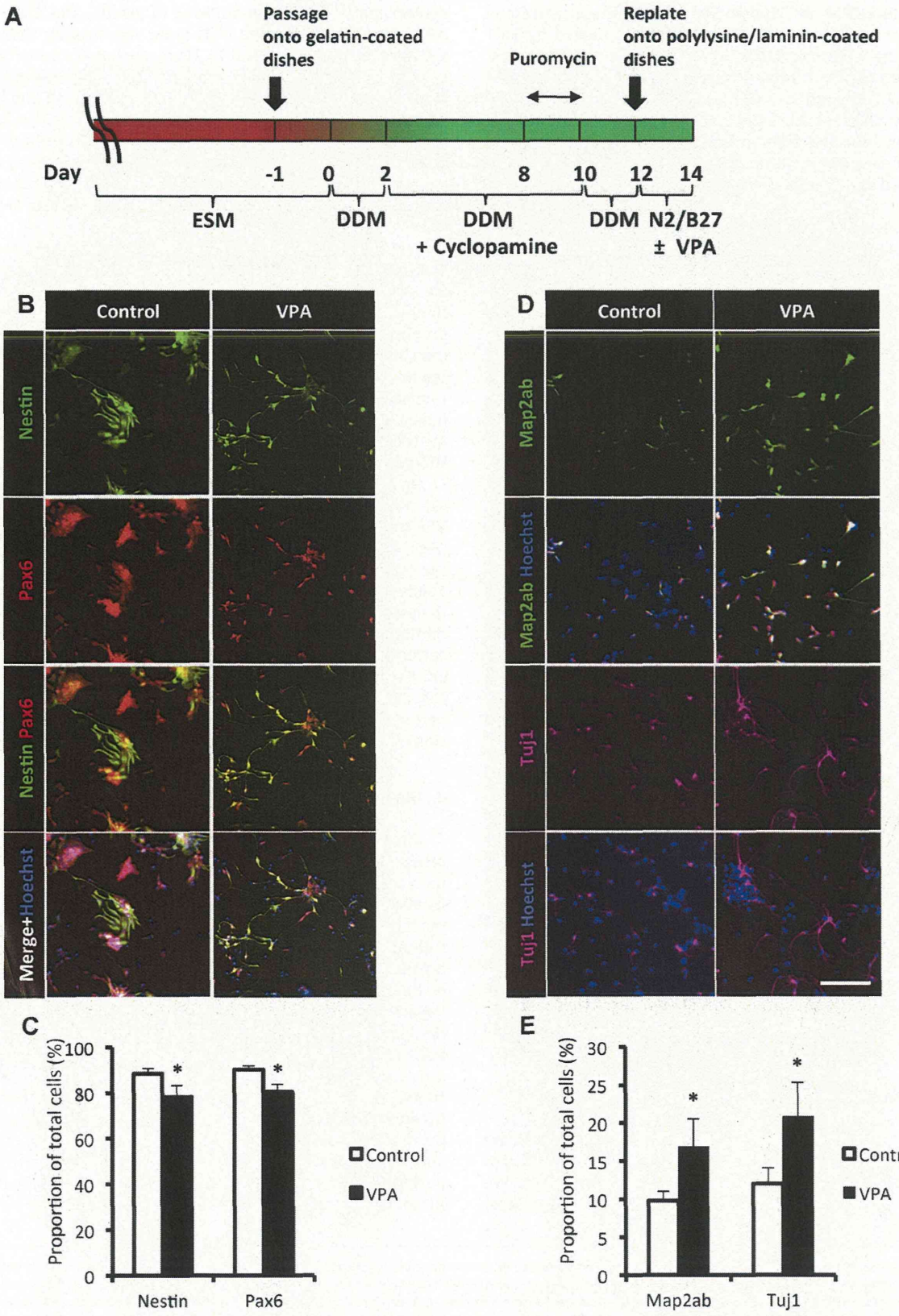
A
Passage
onto gelatin-coated
dishes
Puromycin
Replate
onto polylysine/laminin-coated
dishes
Day
-1
0
2
8
10
12
14
ESM
DDM
DDM
+ Cyclopamine
DDM
N2/B27
± VPA
B
Control
VPA
Nestin
Pax6
Nestin Pax6
Merge+Hoechst
D
Control
VPA
Map2ab
Map2ab Hoechst
Tuj1
Tuj1 Hoechst
C
Proportion of total cells (%)
100
80
60
40
20
0
*
*
Nestin
Pax6
Control
VPA
E
Proportion of total cells (%)
30
25
20
15
10
5
0
*
*
Map2ab
Tuj1
Control
VPA

default medium (DDM) for 10 days (Fig. 1A). We monitored *Sox1*-GFP expression and neuronal differentiation (as judged by Tuj1 immunostaining) each day during this period. We found that 46C mESCs differentiated more slowly into the neural lineage in DDM than in N2/B27. Although *Sox1*-GFP-positive NPCs could already be observed from differentiation day 3, they reached 80% of the total cell population only after differentiation day 8 (Fig. 1B, D, D′, F and F′). We also observed that starting from differentiation day 4, some of the NPCs had already differentiated into neurons (Fig. 1B, E, E′, F and F′).

We next examined the effects of the Shh inhibitor cyclopamine on 46C mESC survival and neural commitment. mESC-derived NPCs in DDM reportedly tend to possess ventral forebrain-like identity, and the addition of cyclopamine converts most of them into dorsal forebrain-like cells without affecting their proliferative pattern (Gaspard et al., 2008). We observed a similar pattern of neural commitment when we cultured 46C mESCs in DDM with or without cyclopamine, and found no significant difference in terms of cell survival (Fig. 1C, G–I and G′–I′). Thus, we conclude that 46C mESCs can survive and differentiate into the neural lineage in DDM with cyclopamine.

3.2. VPA enhances neurogenesis of 46C mESC-derived NPCs

Another advantage of using 46C mESCs is the existence of an internal ribosome entry site (IRES)-linked puromycin resistance gene which was also knocked-in together with GFP-encoding sequence to replace the *Sox1* gene's open reading frame (Ying et al., 2003). Hence, we can enrich the resulting NPCs by addition of puromycin to the medium. Because we found that the majority of 46C mESCs (>80%) had already differentiated into NPCs by differentiation day 8 (Fig. 1B and C), we added puromycin from differentiation day 8 to day 10 for our subsequent analysis.

Next, we examined the differentiation potential of enriched NPCs which were derived from 46C mESCs. We adopted the differentiation protocol of Gaspard et al. (2008, 2009) for making cortical neurons (Figs. 2A and 3A). At differentiation day 14 (Fig. 2A), we found that more than 80% of the cells were nestin- and Pax6-positive, indicating that they were mostly still NPCs (Fig. 2B and C). VPA treatment for 2 days reduced the proportion of cells positive for both markers (Fig. 2B and C). This reduction was accompanied by an increase of Map2ab- and Tuj1-positive neuronal cells (Fig. 2D and E). We then conducted the same analysis for a longer culture period, up to differentiation day 21 (Fig. 3A). We still found higher proportion of neuronal marker-positive (Map2ab+, Tuj1+) cells in the VPA-treated dishes compared with control (Fig. 3B and C). These results indicate that the enrichment of NPCs by puromycin was successful and that VPA treatment enhances neuronal differentiation of these NPCs.

3.3. VPA induces the generation of superficial-layer neurons

Given that neurogenesis was enhanced by VPA treatment, we then looked at the cortical types of these neurons at differentiation day 14 (after two days exposure to VPA; Fig. 2A). We first found a decreased proportion of early born and deep-layer neuron markers. The proportions of reelin- and Ctip2-positive cells among Tuj1-positive cells were significantly decreased by VPA treatment (Fig. 4A and C). Next, we found an increased proportion of superficial-layer marker (Cux1)-positive cells among Map2ab-positive cells after VPA treatment (Fig. 4B and D). When we prolonged the culture until differentiation day 21 (Fig. 3A), we obtained similar results. The proportions of cells positive for early born or deep-layer markers (reelin+, Ctip2+) among Tuj1-positive neuronal cells were still lower (Fig. 5A and C), while that for cells expressing the superficial-layer marker (Cux1+) was also higher, after VPA treatment (Fig. 5B and D).

When we compared the proportions of neurons in control and VPA-treated cell populations at day 14 with those at day 21, we saw a 3-fold increase during this period under both conditions (Figs. 2E and 3C). In control cells, we observed an increased proportion of Ctip2-positive cells among Tuj1-positive cells during this period (Figs. 4C and 5C). In contrast, the proportions of reelin- or Cux1-positive cells among neuronal marker-positive cells remained unchanged (Figs. 4C and D and 5C and D). These results indicate that in control cells, the majority of neurons produced during this period were Ctip2-positive, even though some of the NPCs still generated reelin- and Cux1-positive neurons.

On the other hand, the proportion of cells positive for the cortical markers we tested among neuronal marker-positive cells after VPA treatment did not change during the extended culture period (Figs. 4C and D and 5C and D). This indicates that VPA enhanced the production of Cux1-positive neurons only while it was being applied to the culture (differentiation day 12 to day 14). Nevertheless, the production of Ctip2-positive neurons in VPA treatment diminished compared to that in control cells during the extended culture period. These results suggest that transient VPA treatment enhances the temporal progression of some deep-layer-producing NPCs into superficial-layer-producing types during the treatment period, whereafter the residual NPCs retain this temporal progression even when VPA has been withdrawn from the culture.

4. Discussion

The brains of mammals differ in many aspects from those of other vertebrates. Most striking among the features that mammals have acquired during evolution are the increased size and complexity of the cerebral cortex, the largest brain structure where many of the higher cognitive functions reside (Finlay and Darlington, 1995; Hill and Walsh, 2005). The mammalian cerebral cortex is highly organized, with a six-layered structure that contains early-born or deep-layer (layers I, V and VI) and superficial-layer neurons (layers II–IV) that are produced in an orderly inside-out fashion (Molyneaux et al., 2007). The increased size and complexity partly reflect the overrepresentation of superficial-layer neurons, which are very abundant in primates, and especially so in human (Marin-Padilla, 1992). These cortical neurons are mainly of two types: pyramidal projection neurons, which mostly originate from NPCs of the dorsolateral wall of the telencephalon (Molyneaux et al., 2007), and interneurons, which originate from the ventral telencephalon during embryonic development (Wonders and Anderson, 2006). Although several studies have reported that ESCs can recapitulate

Fig. 2. VPA enhances neurogenesis of 46C mESC-derived NPCs. (A) Timeline of the corticogenesis protocol used for early differentiation analysis. mESCs were routinely propagated and passaged to gelatin-coated dishes in embryonic stem cells medium (ESM) 1 day before neural induction (day −1). The next day (day 0), medium was changed to chemically defined default medium (DDM) and cyclopamine was added from differentiation day 2 to day 10. At differentiation day 12, mESC-derived NPCs were replated to polylysine/laminin-coated dishes in N2/B27 (1:1 mixture of DDM and Neurobasal + B27). Valproic acid (VPA) was added where appropriate at differentiation day 12 and cells were harvested at differentiation day 14. (B–E) Representative immunostaining images from differentiation day 14 of nestin- and Pax6-expressing (green and red, respectively, in B), or Map2ab- and Tuj1-expressing (green and magenta, respectively, in D) cells and their quantification (C and E). Merged images with and without Hoechst (blue in B and D) are also shown. Tuj1 images in D were derived from the triple immunostaining data of Fig. 4A. Data are mean ± SD from at least three independent experiments. *$P < 0.05$ (Student's *t*-test). Scale bar is 100 μm. (For interpretation of the references to color in this figure legend, the reader is referred to the web version of the article.)

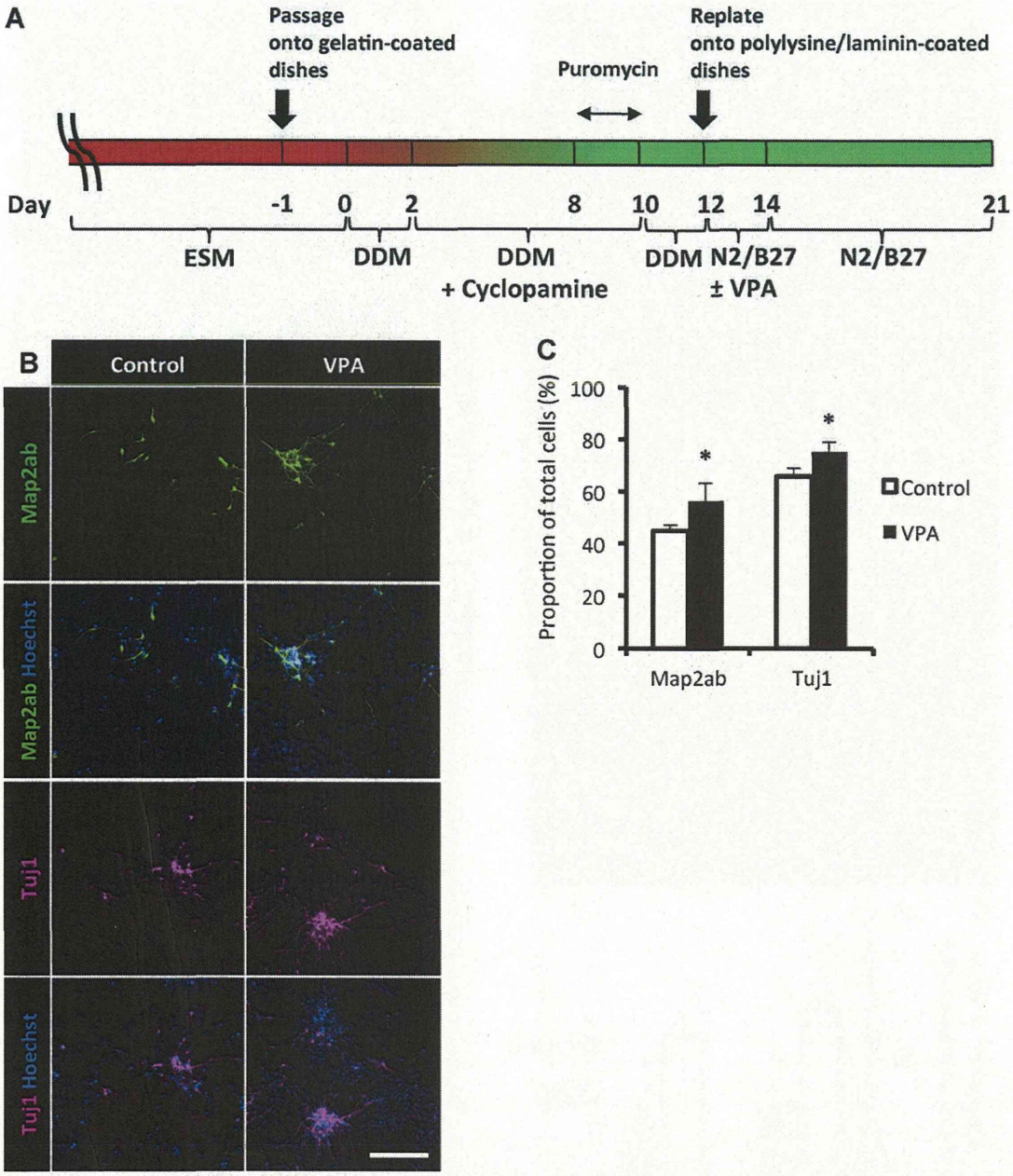

Fig. 3. Increased neurogenesis by VPA is observed even in prolonged culture. (A) Timeline of corticogenesis protocol used for late differentiation analysis. mESCs were routinely propagated and passaged to gelatin-coated dishes in embryonic stem cells medium (ESM) 1 day before neural induction (day −1). The next day (day 0), medium was changed to chemically defined default medium (DDM) and cyclopamine was added from differentiation day 2 to day 10. At differentiation day 12, mESC-derived NPCs were replated to polylysine/laminin-coated dishes in N2/B27 (1:1 mixture of DDM and Neurobasal + B27). Valproic acid (VPA) was added where appropriate at differentiation day 12 and cells were harvested at differentiation day 21. (B) Representative immunostaining images from differentiation day 21 of Map2ab- and Tuj1-expressing (green and magenta, respectively) cells. Merged images with Hoechst (blue) are also shown. Map2ab and Tuj1 images were derived from double- and triple-immunostaining data of Fig. 5A and B, respectively. (C) Quantification of neuronal marker-positive cells found in B. Data are mean ± SD from at least three independent experiments. $^*P < 0.05$ (Student's *t*-test). Scale bar is 100 μm. (For interpretation of the references to color in this figure legend, the reader is referred to the web version of the article.)

certain aspects of cortical neurogenesis *in vitro* (Eiraku et al., 2008; Gaspard et al., 2008), the generation of superficial-layer neurons in those studies was very limited.

In the present study, we have demonstrated that transient HDAC inhibition by VPA in 46C mESC-derived NPCs enhances their neuronal differentiation (Fig. 2D and E). This has been reported previously in several studies using different types of NPCs (Hsieh et al., 2004; Murabe et al., 2007; Yu et al., 2009). Using an mESC culture system that can specifically produce and recapitulate the generation of cortical-layer neurons (Gaspard et al., 2008, 2009), we further showed that the increasing neuronal population after VPA treatment includes a higher proportion of superficial-layer neurons (Cux1+) (Fig. 4B and D), accompanied by a decreasing proportion of early-born or deep-layer neurons (reelin+, Ctip2+) (Fig. 4A and C). Therefore, it is conceivable that VPA enhances the temporal progression of some of deep-layer-producing NPCs into superficial-layer-producing NPCs during the time when VPA was being supplied to the culture. The residual NPCs retained this temporal progression even when VPA was withdrawn from the culture, because we still observed the same proportion of all cortical

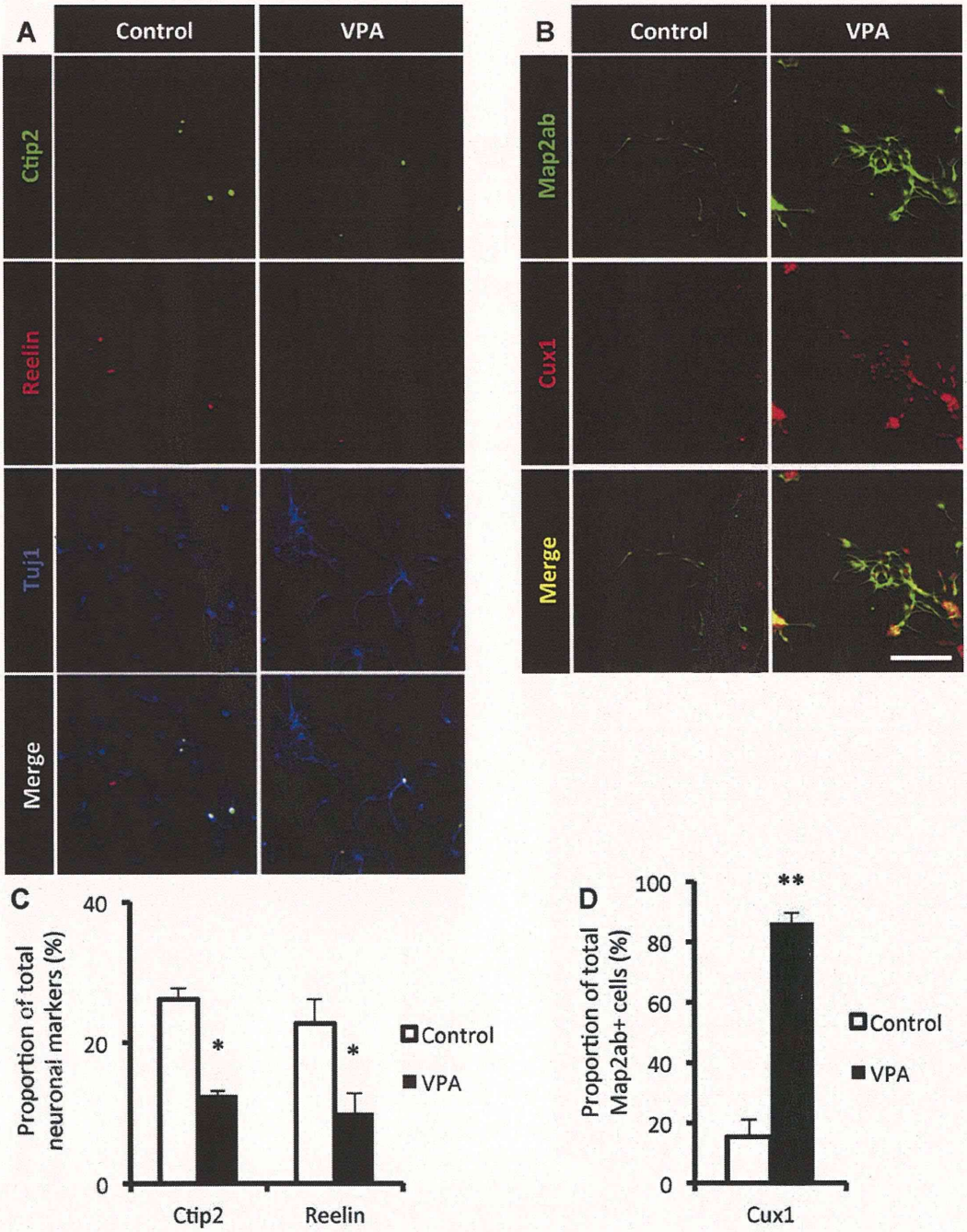

Fig. 4. VPA induces the production of superficial-layer neurons. (A and B) Representative immunostaining images from differentiation day 14, as in Fig. 2A, for Ctip2-, reelin- and Tuj1-expressing (green, red, and blue, respectively, in A), and Map2ab- and Cux1-expressing (green and red, respectively, in B) cells. Merged images are also shown. Hoechst staining can be found in Fig. 2D. Quantification of cortical layer marker-positive cells among neuronal marker-expressing cells for early-born or deep-layer (C) and superficial-layer neurons (D). Data are mean ± SD from at least three independent experiments. $^{*}P < 0.05$, $^{**}P < 0.001$ (Student's *t*-test). Scale bar is 100 μm. (For interpretation of the references to color in this figure legend, the reader is referred to the web version of the article.)

markers even at differentiation day 21, 7 days after VPA treatment was terminated (Fig. 5A–D).

Elucidating the mechanisms that lead to the enhanced progression of NPCs from producing deep-layer neurons to producing superficial-layer neurons after transient VPA treatment is an important challenge for future study. It has been proposed that the zinc-finger transcription factor *Fezf2*, which acts upstream of *Ctip2*, plays an important role in the specification of deep-layer neurons (Chen et al., 2008; Leone et al., 2008). VPA might repress *Fezf2* directly or indirectly in our culture system, which could in turn decrease the generation of deep-layer neurons and release the inhibition of upper-layer neuron production. This scenario is plausible, since VPA treatment of mouse embryos reduces levels of *Fezf2* mRNA in the forebrain (B.J. and K.N., unpublished data), and since there was an increase of Tbr1-positive cells in our culture after VPA treatment (data not shown). It has been reported recently that Tbr1 can act as a direct transcriptional repressor for *Fezf2* (Han et al., 2011).

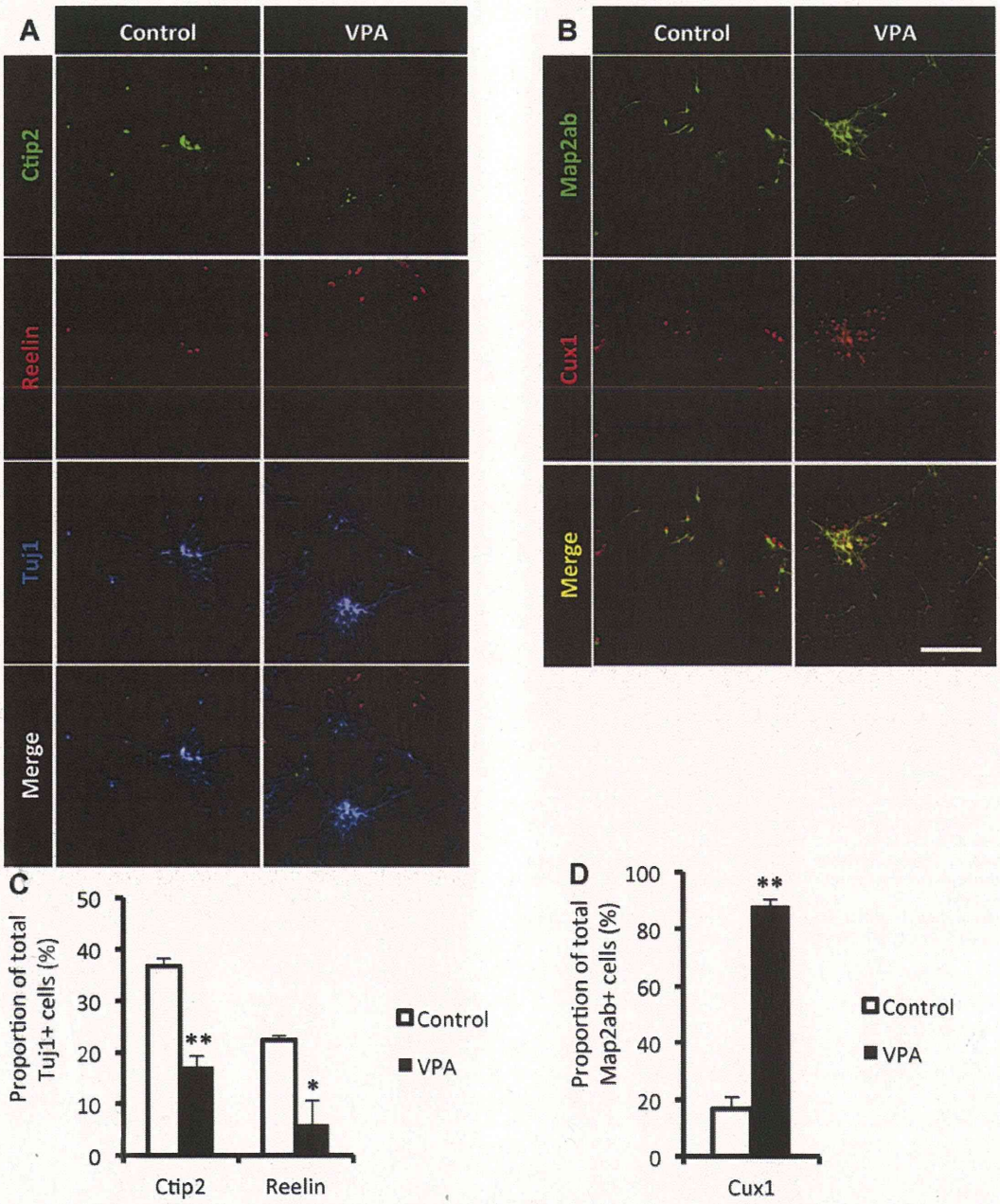

Fig. 5. Increased generation of superficial-layer neurons by VPA is observed even in prolonged culture. (A and B) Representative immunostaining images from differentiation day 21, as in Fig. 3A, for Ctip2-, reelin- and Tuj1-expressing (green, red, and blue, respectively, in A), and Map2ab- and Cux1-expressing (green and red, respectively, in B) cells. Merged images are also shown. Hoechst staining can be found in Fig. 3B. Quantification of cortical layer marker-positive cells among neuronal marker-expressing cells for early-born or deep-layer (C) and superficial-layer neurons (D). Data are mean ± SD from at least three independent experiments. $^{*}P < 0.05$, $^{**}P < 0.001$ (Student's *t*-test). Scale bar is 100 μm. (For interpretation of the references to color in this figure legend, the reader is referred to the web version of the article.)

Our results suggest that histone acetylation plays important roles in the production of superficial-layer neurons in an adherent monolayer system. Similar efficient production of superficial-layer neurons from mESCs was also recently reported in a study of modified embryoid body (EB) formation (Eiraku et al., 2008). It is tempting to hypothesize that in the EB, high levels of histone acetylation occur and persist until late differentiation to help ensure the generation of superficial layer neurons. Nevertheless, generation of cortical neurons from human (h)ESCs using the same EB method was skewed toward deep-layer identity (Eiraku et al., 2008), and both mESCs and hESCs failed to recapitulate the same inside-out pattern of cortical neurogenesis observed in the developing cortex (Au and Fishell, 2008; Gaspard and Vanderhaeghen, 2010). It will be of interest to explore the effects of increasing histone acetylation by VPA treatment on the production of superficial-layer neurons in hESCs, and whether histone acetylation plays a role in the inside-out mode of cortical neurogenesis.

Acknowledgments

We thank Y. Bessho, T. Matsui, Y. Nakahata, J. Kohyama, T. Takizawa and M. Namihira for valuable discussions. We also thank I. Smith for critical reading of the manuscript. We are very grateful to M. Tano for her excellent secretarial assistance and other

laboratory members for technical help. This research was supported in part by Grant-in-Aid for Scientific Research on Innovative Area: NAIST Global COE Program (Frontier Biosciences: Strategies for survival and adaptation in a changing global environment) from the Ministry of Education, Culture, Sports, Science and Technology of Japan; Grant-in-Aid for Scientific Research on Innovative Area: Neural Diversity and Neocortical Organization from the Ministry of Education, Culture, Sports, Science and Technology of Japan; Health Sciences Research Grants from the Ministry of Health, Labour and Welfare, Japan; and Research Fellowships for Young Scientists from the Japan Society for the Promotion of Science.

References

Abranches, E., Silva, M., Pradier, L., Schulz, H., Hummel, O., Henrique, D., Bekman, E., 2009. Neural differentiation of embryonic stem cells *in vitro*: a road map to neurogenesis in the embryo. PLoS ONE 4, e6286.

Au, E., Fishell, G., 2008. Cortex shatters the glass ceiling. Cell Stem Cell 3, 472–474.

Bain, G., Kitchens, D., Yao, M., Huettner, J.E., Gottlieb, D.I., 1995. Embryonic stem cells express neuronal properties *in vitro*. Dev. Biol. 168, 342–357.

Balasubramaniyan, V., Boddeke, E., Bakels, R., Küst, B., Kooistra, S., Veneman, A., Copray, S., 2006. Effects of histone deacetylation inhibition on neuronal differentiation of embryonic mouse neural stem cells. Neuroscience 143, 939–951.

Chen, B., Wang, S.S., Hattox, A.M., Rayburn, H., Nelson, S.B., McConnell, S.K., 2008. The Fezf2-Ctip2 genetic pathway regulates the fate choice of subcortical projection neurons in the developing cerebral cortex. Proc. Natl. Acad. Sci. U. S. A. 105, 11382–11387.

Conti, L., Pollard, S.M., Gorba, T., Reitano, E., Toselli, M., Biella, G., Sun, Y., Sanzone, S., Ying, Q.L., Cattaneo, E., Smith, A., 2005. Niche-independent symmetrical self-renewal of a mammalian tissue stem cell. PLoS Biol. 3, e283.

Eiraku, M., Watanabe, K., Matsuo-Takasaki, M., Kawada, M., Yonemura, S., Matsumura, M., Wataya, T., Nishiyama, A., Muguruma, K., Sasai, Y., 2008. Self-organized formation of polarized cortical tissues from ESCs and its active manipulation by extrinsic signals. Cell Stem Cell 3, 519–532.

Finlay, B.L., Darlington, R.B., 1995. Linked regularities in the development and evolution of mammalian brains. Science 268, 1578–1584.

Gaspard, N., Bouschet, T., Hourez, R., Dimidschstein, J., Naeije, G., van den Ameele, J., Espuny-Camacho, I., Herpoel, A., Passante, L., Schiffmann, S.N., Gaillard, A., Vanderhaeghen, P., 2008. An intrinsic mechanism of corticogenesis from embryonic stem cells. Nature 455, 351–357.

Gaspard, N., Bouschet, T., Herpoel, A., Naeije, G., van den Ameele, J., Vanderhaeghen, P., 2009. Generation of cortical neurons from mouse embryonic stem cells. Nat. Protoc. 4, 1454–1463.

Gaspard, N., Vanderhaeghen, P., 2010. Mechanisms of neural specification from embryonic stem cells. Curr. Opin. Neurobiol. 20, 37–43.

Guillemot, F., Molnár, Z., Tarabykin, V., Stoykova, A., 2006. Molecular mechanisms of cortical differentiation. Eur. J. Neurosci. 23, 857–868.

Han, W., Kwan, K.Y., Shim, S., Lam, M.M., Shin, Y., Xu, X., Zhu, Y., Li, M., Sestan, N., 2011. TBR1 directly represses Fezf2 to control the laminar origin and development of the corticospinal tract. Proc. Natl. Acad. Sci. U. S. A. 108, 3041–3046.

Hill, R.S., Walsh, C.A., 2005. Molecular insights into human brain evolution. Nature 437, 64–67.

Hsieh, J., Nakashima, K., Kuwabara, T., Mejia, E., Gage, F.H., 2004. Histone deacetylase inhibition-mediated neuronal differentiation of multipotent adult neural progenitor cells. Proc. Natl. Acad. Sci. U. S. A. 101, 16659–16664.

Juliandi, B., Abematsu, M., Nakashima, K., 2010. Chromatin remodeling in neural stem cell differentiation. Curr. Opin. Neurobiol. 20, 408–415.

Kawasaki, H., Mizuseki, K., Nishikawa, S., Kaneko, S., Kuwana, Y., Nakanishi, S., Nishikawa, S.I., Sasai, Y., 2000. Induction of midbrain dopaminergic neurons from ES cells by stromal cell-derived inducing activity. Neuron 28, 31–40.

Leone, D.P., Srinivasan, K., Chen, B., Alcamo, E., McConnell, S.K., 2008. The determination of projection neuron identity in the developing cerebral cortex. Curr. Opin. Neurobiol. 18, 28–35.

Marin-Padilla, M., 1992. Ontogenesis of the pyramidal cell of the mammalian neocortex and developmental cytoarchitectonics: a unifying theory. J. Comp. Neurol. 321, 223–240.

Molyneaux, B.J., Arlotta, P., Menezes, J.R.L., Macklis, J.D., 2007. Neuronal subtype specification in the cerebral cortex. Nat. Rev. Neurosci. 8, 427–437.

Murabe, M., Yamauchi, J., Fujiwara, Y., Hiroyama, M., Sanbe, A., Tanoue, A., 2007. A novel embryotoxic estimation method of VPA using ES cells differentiation system. Biochem. Biophys. Res. Commun. 352, 164–169.

Pevny, L.H., Sockanathan, S., Placzek, M., Lovell-Badge, R., 1998. A role for SOX1 in neural determination. Development 125, 1967–1978.

Shen, Q., Wang, Y., Dimos, J.T., Fasano, C.A., Phoenix, T.N., Lemischka, I.R., Ivanova, N.B., Stifani, S., Morrisey, E.E., Temple, S., 2006. The timing of cortical neurogenesis is encoded within lineages of individual progenitor cells. Nat. Neurosci. 6, 743–751.

Wiles, M.V., Johansson, B.M., 1999. Embryonic stem cell development in a chemically defined medium. Exp. Cell Res. 247, 241–248.

Wonders, C.P., Anderson, S.A., 2006. The origin and specification of cortical interneurons. Nat. Rev. Neurosci. 7, 687–696.

Wood, H.B., Episkopou, V., 1999. Comparative expression of the mouse Sox1, Sox2 and Sox3 genes from pre-gastrulation to early somite stages. Mech. Dev. 86, 197–201.

Ying, Q.L., Smith, A.G., 2003. Defined conditions for neural commitment and differentiation. Methods Enzymol. 365, 327–341.

Ying, Q.L., Stavridis, M., Griffiths, D., Li, M., Smith, A., 2003. Conversion of embryonic stem cells into neuroectodermal precursors in adherent monoculture. Nat. Biotechnol. 21, 183–186.

Yu, I.T., Park, J.Y., Kim, S.H., Lee, J.S., Kim, Y.S., Son, H., 2009. Valproic acid promotes neuronal differentiation by induction of proneural factors in association with H4 acetylation. Neuropharmacology 56, 473–480.

STEM CELLS®
REGENERATIVE MEDICINE

Treatment of a Mouse Model of Spinal Cord Injury by Transplantation of Human Induced Pluripotent Stem Cell-Derived Long-Term Self-Renewing Neuroepithelial-Like Stem Cells

YUSUKE FUJIMOTO,[a,b] MASAHIKO ABEMATSU,[b] ANNA FALK,[c] KEITA TSUJIMURA,[a] TSUKASA SANOSAKA,[a] BERRY JULIANDI,[a,d] KATSUNORI SEMI,[a] MASAKAZU NAMIHIRA,[a] SETSURO KOMIYA,[b] AUSTIN SMITH,[c] KINICHI NAKASHIMA[a]

[a]Laboratory of Molecular Neuroscience, Graduate School of Biological Sciences, Nara Institute of Science and Technology, Ikoma, Japan; [b]Department of Orthopaedic Surgery, Graduate School of Medical and Dental Sciences, Kagoshima University, Kagoshima, Japan; [c]Department of Biochemistry, Wellcome Trust Centre for Stem Cell Research, Stem Cell Institute, University of Cambridge, Cambridge, United Kingdom; [d]Department of Biology, Bogor Agricultural University (IPB), Bogor, Indonesia

Key Words. Spinal cord injury • Induced pluripotent stem cells • Neural stem cells • Transplantation • Regenerative medicine

ABSTRACT

Because of their ability to self-renew, to differentiate into multiple lineages, and to migrate toward a damaged site, neural stem cells (NSCs), which can be derived from various sources such as fetal tissues and embryonic stem cells, are currently considered to be promising components of cell replacement strategies aimed at treating injuries of the central nervous system, including the spinal cord. Despite their efficiency in promoting functional recovery, these NSCs are not homogeneous and possess variable characteristics depending on their derivation protocols. The advent of induced pluripotent stem (iPS) cells has provided new prospects for regenerative medicine. We used a recently developed robust and stable protocol for the generation of long-term, self-renewing, neuroepithelial-like stem cells from human iPS cells (hiPS-lt-NES cells), which can provide a homogeneous and well-defined population of NSCs for standardized analysis. Here, we show that transplanted hiPS-lt-NES cells differentiate into neural lineages in the mouse model of spinal cord injury (SCI) and promote functional recovery of hind limb motor function. Furthermore, using two different neuronal tracers and ablation of the transplanted cells, we revealed that transplanted hiPS-lt-NES cell-derived neurons, together with the surviving endogenous neurons, contributed to restored motor function. Both types of neurons reconstructed the corticospinal tract by forming synaptic connections and integrating neuronal circuits. Our findings indicate that hiPS-lt-NES transplantation represents a promising avenue for effective cell-based treatment of SCI. STEM CELLS *2012;30:1163–1173*

Disclosure of potential conflicts of interest is found at the end of this article.

INTRODUCTION

Our current ability to reconstruct the damaged central nervous system, including spinal cord injury (SCI), is limited. SCI is one of the commonest causes of loss of movement and sensation below the level of the injured spinal cord. While partial spontaneous functional recovery has been observed in the case of moderate SCI, there is no adequate treatment to repair the injured spinal cord itself, and most patients have no therapeutic options except for general management and rehabilitation [1].

Transplantation of neural stem cells (NSCs) into the injured spinal cord has been shown to be an effective treatment [2] because of their competence to differentiate into neurons and oligodendrocytes and to secrete neurotrophic factors. Transplantation into injured spinal cords of several different types of human NS/progenitor cells, derived from human fetal tissue [3, 4] or from human embryonic stem cells (hESCs) [5, 6], promotes functional recovery in animal models. Nonetheless, the mechanism underlying such functional improvement remains to be fully elucidated.

The establishment of induced pluripotent stem cells (iPSCs) offers new prospects for regenerative therapies [7, 8]. Human iPSCs (hiPSCs) can be generated from cells in adult tissue, making it possible to create iPSCs from SCI patients themselves. From the viewpoint of ethics and host immune rejection, NSCs derived from human iPSCs (hiPS-NSCs)

Author contributions: Y.F.: conception and design, collection and assembly of data, data analysis and interpretation, and manuscript writing; A.F. and A.S.: provision of study materials; M.A., K.T., T.S., K.S., and M.N.: collection and assembly of data, data analysis and interpretation; B.J.: manuscript writing; S.K.: administrative support; K.N.: conception and design, administrative support, manuscript writing, and final approval of manuscript.

Correspondence: Kinichi Nakashima, Ph.D., Laboratory of Molecular Neuroscience, Graduate School of Biological Sciences, Nara Institute of Science and Technology, 8916-5 Takayama, Ikoma 631-0192, Japan. Telephone: 81-743-72-5471; Fax: 81-743-72-5479; e-mail: kin@bs.naist.jp. Received October 18, 2011; accepted for publication February 11, 2012; first published online in STEM CELLS *EXPRESS* March 14, 2012. 1066-5099/2012/$30.00/0 doi: 10.1002/stem.1083

appear to be an ideal resource for transplantation therapy, and the efficacy of hiPS-NSC transplantation in SCI treatment has just begun to be investigated using the mouse model of SCI [9].

We used a recently developed protocol for the generation of long-term self-renewing neuroepithelial-like stem (lt-NES) cells, which satisfy the criteria to be defined as NSCs, from several different lines of hESCs and hiPSCs [10, 11]. hiPSC-derived lt-NES (hiPS-lt-NES) cells exhibit consistent characteristics such as continuous expandability, stable neuronal and glial differentiation ability, and the capacity to generate functional mature neurons in monolayer culture. Whereas neurosphere cultures display heterogeneous character and are sensitive to variation in methodological procedures [12], monolayer cultures offer a more homogeneous and robust cell generation [13, 14].

We report here that transplanted hiPS-lt-NES cells, derived from our robust and stable monolayer cultures, have a therapeutic potential comparable to that of NSCs from human fetal spinal cord (hsp-NSCs) for SCI in the nonobese diabetic-severe combined immunodeficient (NOD-SCID) mouse model. We further show that hiPS-lt-NES cell transplantation promotes recovery of hind limb motor function through the reconstruction of the corticospinal tract (CST), and restores disrupted neuronal circuitry in a relay manner as we have previously demonstrated in a study of mouse NSC transplantation [15]. Our results suggest that hiPS-lt-NES cells represent a promising cell source for transplantation into the injured spinal cord.

Materials and Methods

Cell Culture

hsp-NSCs and hiPS-lt-NES cells were established and maintained as described previously [10, 11, 16]. The hsp-NS cell line CB660sp and hiPS-lt-NES cell line AF22 were used in the present study. hsp-NSCs were plated onto 10 μg/ml laminin (Sigma, St. Louis, MO, http://www.sigmaaldrich.com)-coated plates in maintenance medium, consisting of Euromed-N medium (Euroclone, Milano, Italy, http://www.euroclonegroup.it), 2 mM L-glutamine, 0.1 mg/ml penicillin/streptomycin (Sigma), N2 supplement (1:100), 20 ml/l B27 (all from Invitrogen, Carlsbad, CA, http://www.invitrogen.com), 10 ng/ml fibroblast growth factor (FGF, R&D Systems, Minneapolis, MN, http://www.rndsystems.com)-2, and 10 ng/ml epidermal growth factor (EGF, R&D Systems). Cells were passaged at a ratio of 1:2 every second to third day using Accutase (Sigma). hiPS-lt-NES cells were plated onto 0.1 mg/ml poly-L-ornithine and 10 μg/ml laminin (O/L, Sigma)-coated plates in maintenance medium, consisting of Dulbecco's modified Eagle's medium/F12 (Invitrogen), 2 mM L-glutamine, 1.6 mg/ml glucose, 0.1 mg/ml penicillin/streptomycin, N2 supplement (1:100), 1 μl/ml B27, 10 ng/ml FGF2 and 10 ng/ml EGF. Cells were passaged at a ratio of 1:3 every second to third day using trypsin. To induce in vitro differentiation, hiPS-lt-NES cells were plated onto an O/L-coated 35-mm dish at a density of 5×10^5 cells per dish in culture medium without both EGF and FGF, containing 1% fetal bovine serum (FBS), and cultured for 4 weeks. Half of the medium was changed every 2 days and laminin (1:500) was added to the medium once a week to prevent detachment of the cells.

Lentivirus Production and Infection of hsp-NSCs and hiPS-Lt-NES Cells

Lentivirus production and infection of cells were performed as described previously [17, 18]. hsp-NSCs and hiPS-lt-NES cells were infected with lentiviruses harboring the luciferase and green fluorescent protein (GFP) genes connected by an internal ribosomal entry site (IRES), EFp (elongation factor promoter)-luciferase-IRES-GFP (Fig. 1B). hsp-NSCs and hiPS-lt-NES cells that had undergone more than 20 passages were infected. GFP-positive cells were collected by fluorescence activated cell sorting (FACS)-Aria II CellSorter (B.D. Biosciences, San Jose, CA, http://www.bdbiosciences.com) and used for transplantation.

SCI Model and Cell Transplantation

All aspects of animal care and treatment were carried out according to the guidelines of the experimental animal care committee of Nara Institute of Science and Technology. We used female NOD-SCID mice (8-10 weeks old, weighing 18-20 g, Charles River, Osaka, Japan, http://www.crj.co.jp). Anesthetized (ketamine 50 mg/kg, xylazine 5 mg/kg, and sodium pentobarbital 20 mg/kg) mice received laminectomies and partial laminectomies at the ninth and 10th thoracic spinal vertebrae, respectively. The dorsal surface of the dura mater was exposed and SCI was induced using an SCI device (70 kdyn; Infinite Horizon impactor, Precision Systems & Instrumentation, Lexington, KY, http://www.presysin.com) as previously described [15]. The muscle and skin were closed in layers. All mice subcutaneously received gentamicin (8 mg/kg) daily. The mice underwent manual bladder evacuation once a day. Seven days after injury, mice were anesthetized and transplanted with hiPS-lt-NES cells or hsp-NSCs using a glass micropipette attached to a stereotaxic injector (Narishige, Tokyo, Japan, http://www.narishige.co.jp). The tip of the micropipette was inserted into the injury epicenter in the injured spinal cord, and 2 μl of culture medium lacking growth factors, with or without NSCs (5×10^5 μl^{-1}), was injected at a rate of 1 μl/min.

Behavioral Testing and Electrophysiological Recordings

We evaluated the motor function of the hind limbs for up to 10 weeks after injury. Two individuals, blinded to the treatment of the mice, examined motor function using the Basso Mouse Scale (BMS) locomotor rating scale [19]. Hind limb movements of the mice were captured using a high-definition digital camcorder. We edited these movies and exported movie files using editing software.

To examine signal conduction in motor pathways after SCI, motor-evoked potentials (MEPs) at 12 weeks after SCI were measured. Mice were anesthetized with intraperitoneally injected ketamine (100 mg/kg) and their heads were fixed in a stereotactic frame. The skulls were tightly fixed to a stereotaxic apparatus (Narishige). Scalping and two small craniotomies were performed with a drill over the motor cortex area (Nakanishi, Tochigi, Japan; http://www.nsk-nakanishi.co.jp). Silver ball electrodes were placed epidurally via the holes, into which mineral oil was applied. The motor cortex was stimulated with 0.2-msecond square wave pulses at a constant current of 10 mA using an electrical stimulator (SEM-3301, Nihon Kohden, Tokyo, Japan; http://www.nihonkohden.co.jp). Recording needle electrodes were inserted into the hamstring. A subcutaneous ground electrode was placed in the tail. Electrophysiological recordings were made (MED64, Alpha MED Scientific, Osaka, Japan; http://www.amedsci.com) and band-pass filtered at 1-10 kHz. Amplitudes from onset to peak of the negative deflection were measured. Latency of MEP was measured as the time interval between the end of stimulation and the onset of the first wave. Indicated values are the average of five experiments from each mouse.

Antibodies

The following antibodies were used: rabbit anti-Sox2 (1:1,000, Chemicon-Millipore, Billerica, MA, http://www.millipore.com), mouse anti-Nestin (1:250, Chemicon), rabbit anti-brain lipid-binding protein (BLBP, 1:500, Abcam, Cambridge, U.K., http://www.abcam.com), mouse anti-β-tubulin isotype III (Tuj1; 1:500,